Research Paper

Identification and validation of methylation-CpG prognostic signature for prognosis of hepatocellular carcinoma

Chunmei He[1,3,*], Zehao Guo[1,2,*], Hao Zhang[1,2], Ganqing Yang[1], Jintao Gao[1,2], Zhijing Mo[1,2]

[1]School of Intelligent Medicine and Biotechnology, Guilin Medical University, Guilin 541199, Guangxi, China
[2]Key Laboratory of Biochemistry and Molecular Biology (Guilin Medical University), Education Department of Guangxi Zhuang Autonomous Region, Guilin 541199, Guangxi, China
[3]Chandi Precision Medical Technology, Foshan 528000, Guangdong, China
*Equal contribution

Correspondence to: Zhijing Mo, Jintao Gao, Ganqing Yang; **email:** mozhijing@glmc.edu.cn, jintao_gao@glmc.edu.cn, yangganqing@glmc.edu.cn
Keywords: hepatocellular carcinoma, prognostic, methylation, oxidative stress, immune checkpoint
Received: May 8, 2023 **Accepted:** December 6, 2023 **Published:** January 18, 2024

ABSTRACT

Epigenetic biomarkers help predict the prognosis of cancer patients and evaluating the clinical outcome of immunization therapy. In this study, we present a personalized gene methylation-CpG signature to enhance the accuracy of survival prediction for individuals with hepatocellular carcinoma (HCC). Utilizing RNA sequencing and methylation datasets from GEO as well as TCGA, we conducted single sample GSEA (ssGSEA), WGCNA, as well as Cox regression. Through these analyses, we identified 175 oxidative stress and immune-related genes along with 4 CpG loci that are associated with the prognosis of HCC. Subsequently, we constructed a prognostic signature for HCC utilizing these 4 CpG sites, referred to as the HCC Prognostic Signature of Methylation-CpG sites (HPSM). Further investigation revealed an enrichment of immune-related signal pathways in the HPSM-low group, which demonstrated a positive correlation with better survival among HCC patients. Moreover, the methylation of the CpG sites in HPSM was found to be closely linked to drug sensitivity. *In vitro* experiments tentatively confirmed that promoter methylation regulated the expression of BMPER, one of the CpG sites within HPSM. The expression of BMPER was significantly correlated with cell death in the oxidative stress pathway, and overexpression of BMPER effectively inhibited HCC cell proliferation. Consequently, our findings suggest that HPSM is an independent predictive factor and holds promise for accurately predicting the prognosis of HCC patients.

INTRODUCTION

Hepatocellular carcinoma (HCC) is a common cancer with high recurrence and mortality rates [1]. Increasing research has demonstrated that oxidative stress exerts a pivotal effect in the advancement of HCC [2, 3]. Additionally, abnormal gene functioning resulting from DNA methylation has been linked to cancer initiation, progression, and drug resistance [4–6]. Many studies have reported that oxidative stress can lead to abnormal hypermethylation and inactivation of tumor suppressor genes, contributing to carcinogenesis [7–9]. Therefore, methylation and oxidation-related markers may have potential effects on HCC occurrence and development. However, these markers lack perfection when predicting treatment efficacy.

The methylation of DNA is a pivotal epigenetic inheritance adorn that influences gene expression and

chromosomal stability, thus contributing to tumor genesis and development. Current research on liver cancer methylation primarily focuses on differences in whole genome methylation of DNA profiles and the application of methylation markers in liver cancer detection. Targeted molecular therapy is currently a prominent area of investigation in liver cancer research [10, 11]. Recent studies have revealed that oncogene-induced oxidative stress is a key driver of CpG island hypermethylation [9, 12]. Identifying methylation markers that predict immune response and prognosis will facilitate personalized immunotherapy for HCC patients [13, 14]. Despite extensive investigation into immune-related molecular functions and interactions, there is limited research on their epigenetic regulation [15]. Gaining insight into the regulation and control of immune checkpoint genes is crucial for developing mechanistically-driven biomarkers to predict immuno-therapy response. In this exploration, we employed WGCNA, single-sample GSEA (ssGSEA) analysis, as well as Cox regression to identify 175 oxidative stress and immune-related genes and 4 CpG sites associated with HCC prognosis. With these four CpG sites, we constructed the HCC Prognostic Signature of Methylation-CpG sites (HPSM), and analyzed the molecular and immune characteristics discrepancies between the HPSM-low and HPSM-high groups. Furthermore, we performed drug sensitivity analysis on the CpG sites of HPSM. Additionally, we confirmed *in vitro* the relationship between methylation of one of the CpG sites within the BMPER gene contained in HPSM and its biological function in HCC gene expression. Constructing HPSM for HCC patients may uncover underlying mechanisms between methylation and oxidative stress and the prognosis of individuals affected by HCC.

MATERIALS AND METHODS

Data capture

RNA-seq data from 424 HCC specimens, including 374 cancerous and 50 adjacent normal tissue specimens, along with clinicopathological information, single nucleotide variations, and 450K methylation data, were obtained from The Cancer Genome Atlas (TCGA) (http://www.cbioportal.org/). Additionally, the GSE52018, GSE14520, and GSE 57956 datasets were retrieved from GEO data-base (https://www.ncbi.nlm.nih.gov/geo/). Patients with incomplete pathological data were excluded. The drug sensitivity file "compound activity: DTP NCI-60" and the drug methylation matrix file Illumina 450K methylation were downloaded from the Cell Miner datasets (https://discover.nci.nih.gov/cellminer).

Identification of oxidative stress and immune related genes and prognosis-related CpG sites

Differentially expressed genes (DEGs) as well as differentially methylated genes (DMGs) among the adjacent normal tissues as well as HCC tissues in the GSE14520 and GSE57956 datasets were analyzed using GEO2R. TCGA-LIHC mRNA expression data was also analyzed using R's edge packet analysis, and DEGs were identified based on a threshold of $p < 0.05$ and $|\log 2 \text{ fold change (FC)}| > 1$ with statistical significance. In total, 1203 overlapping genes were got from DEGs along with DMGs. The correlation of these genes with immune and oxidative stress pathways was determined using the ssGSEA package [16] in R. After conducting GO enrichment analysis, 175 oxidative stress and immune-related genes were selected based on a correlation coefficient $> |3|$ and p-value < 0.05. Next, univariate Cox regression analysis was carried out to explore the link of the methylation of CpG sites within these genes and overall survival (OS), filtering out prognosis-related CpG sites using a p-value threshold of less than 0.05.

WGCNA

Co-expression networks were constructed using the "WGCNA" package in R with the overlapping genes identified from the DEGs and DMGs. Outliers were removed, and a similarity expression matrix was established by calculating the Pearson correla-tion coefficient between gene pairs. A soft threshold power of $\beta = 4$ was utilized to construct an adjacency matrix. The topological overlap matrix was obtained by calculating TOM values between pairwise genes. Hierarchical clustering was performed to define modules, and module-trait association analysis was established between cancer and normal phenotypes.

Construction of HPSMs

Data normalization and conversion of DNA methylation from Beta-values to M-values were carried out utilizing the minfi package in R 4.2.2 [17]. A total of 371 HCC patients from TCGA were stochastically allocated into a training set (N=186) as well as a testing dataset (N=185). Single-variable Cox regression analysis was utilized for the screening of prognosis-related CpG sites, considering those with $p < 0.05$ as having prognostic value. To analyze the combined effect of multiple factors, multivariate Cox regression analysis was carried out using the LASSO method to account for multicollinearity. This step further screened candidate CpG sites. Ultimately, four CpG sites were selected as prognostic predictors for HCC, and the HPSM was constructed. A risk scoring formula was developed:

Risk score = (M-value of CpG1) × coef (CpG1) + (M-value of CpG2) × coef (CpG2) + … + (M-value of CpGn) × coef (CpGn). Individuals with HCC were allocated into HPSM-high / HPSM-low groups using the median hazard threshold. Different HPSM subgroups' OS was evaluated utilizing the Kaplan-Meier method as well as log-rank test. The performance of HPSM was evaluated by applying it to the testing dataset, generating a rROC curve, and calculating the AUC.

Gene set enrichment analysis (GSEA) and immune characteristics analysis of HPSM subgroups

GSEA software and the clusterProfiler package in R were used to identify gene sets enriched in the HPSM-high/HPSM-low groups. The gene sets c2.all.v2023.1.Hs. symbols, immunesigdb. v2023.1.Hs. symbols and c5.go.v7.4, symbols were utilized. A false discovery rate (FDR) $q < 0.05$ was indicated to be statistically significant. The tumor-infiltrating immune cell subsets, immune-related functions, and tumor mutation burden (TMB) between the HPSM subgroups were estimated using the ssGSEA package [18] in R 4.2.2 and the maftools package in R 4.2.2.

Independent prognostic analysis and generation of a nomogram

Univariate and multivariate Cox regression analyses were operated utilizing the survival package in R 4.2.2 to evaluate HPSMs' prognostic value. Clinical characteristics such as age, gender, T, N, M, PD-1, TP53 and TMB were included as clinical-pathological covariates [19–21]. A nomogram incorporating T, M, programmed cell death 1 (PDCD1), and HPSM was constructed to forecast OS at 1, 2, and 3 years. The predictive capability together with the accuracy of the nomogram were evaluated using a ROC curve.

Cell culture methods and 5-aza-2'-deoxycytidine treatment strategy

PLC/PRF/5 and Hep3B cell lines were subjected to DMEM medium supplemented with 10% FBS (Gibco, USA) and cultured at the temperature of 37° C with 5% CO_2. For the treatment of PLC/PRF/5 cells, a confirmed DNA methylation inhibitor, 5-aza-2′-deoxycytidine (5-aza-dC) at 4μM, was used [22], Hep3B cells were treated with 5μM 5-aza-dC (Omega Bio-Tek, USA). The culture medium containing 5-aza-dC was replaced daily for three consecutive days.

Bisulfite sequencing PCR (BSP)

BSP was performed to examine the methylation level of the BMPER promoter. The BSP primer sequences used were as follows: forward primer – GTGTGTCGCTCC TTCCCAAAGGTG and reverse primer – GCCCTGG GGCCCTGGCCTCC. Genomic DNA from Hep3B and PLC/PRF/5 cells was extracted using the DNA extraction kit (Omega Bio Tek). Ten randomly selected positive clones were sequenced, and the sequencing results were visualized using SeqMan software.

Quantitative PCR (qPCR)

Total RNA was extracted utilizing TRIzol reagent (TIANGEN, Beijing, China). qPCR was performed to detect the expression of BMPER. The qPCR was carried out using the BioRad CFX96 system and SYBR Green Chemistry (BioRad, USA). The primer sequences for BMPER and GAPDH were as follows: BMPER forward -GAGCCTTGTGTTCTACGCCAGT, BMPER reverse - TACATTTGCTTCCTTCTGGCTGA, GAPDH as an internal reference forward – CATGAGAAGTA TGACAACAGCCT, and GAPDH reverse - AGT CCTTCCACGATACCAAAGT. All primer sequences were obtained from BGI (Hong Kong).

Western blotting (WB)

WB was carried out as described previously [4–6]. Anti-BMPER and anti-β-actin antibodies were purchased from ImmunoWay (USA) and Wanleibio (Shenyang, China).

Stable expression of BMPER using lentiviral vectors

LV-BMPER (BMPER overexpression) and LV-NC (negative control) lentiviral vectors were obtained from Genechem (GENECHEM, Shanghai, China). HCC cells were infected with the lentivirus for 72 hours, followed by treatment with puromycin (Biotopped, Beijing, China). The expression levels of BMPER were detected using WB assays.

Cell proliferation assays

Hep3B cells were seeded in 96-well plates with 5.0×10^3 cells for each well, followed by incubation for 24, 48, 72, and 96 hours. After that, the cells were treated with MTT (5 mg/ml; Sigma, Dorset, UK) for 4 hours. The measurement of optical density (OD) value of each well was performed at 490nm utilizing a microplate reader.

Clone formation assays

Paraformaldehyde and Giemsa were purchased from China National Medicines Corporation, Ltd. (Shanghai, China) and Nanjing Jiancheng Technology Company (Nanjing, China), respectively. LV-NC or LV-BMPER

cells were inoculated into a 6-well plate with 500 cells/well for 10 days. Cells were fixed with 4% paraformaldehyde for a duration of 10 minutes, and then stained with 0.1% Giemsa for a duration of 10 minutes. Cell colonies were then photographed and counted. These experiments were repeated three times independently.

Statistical analysis

Data were presented as mean ± standard deviation. The association between HPSM groups and clinicopathological characteristics was assessed using a Chi-square test. Two-group comparisons (two-tailed) were analyzed using Student's t-test, while one-way analysis of variance (ANOVA) was utilized for comparisons involving more than two groups. Analysis of Pearson correlation was performed. The predictive efficiency of the survival risk score was evaluated using the ROC curve. Univariate and multivariate Cox regression analyses were conducted to predict the variables for the prognosis and clinicopathological characteristics. Data analyses were carried out based on GraphPad Prism 8.0 software together with R 4.0.2. $P < 0.05$ indicated statistically significant.

Availability of data and materials

The datasets of this article were generated from the TCGA database and the GEO database.

RESULTS

WGCNA of DEGs and DMGs in HCC

We obtained a total of 11,045 DEGs from the GSE14520 dataset and 8,029 DMGs from the GSE57956 dataset using GEO2R. Additionally, we evaluated 6,219 DEGs in the TCGA-LIHC RNA-seq expression profile. Among these, we identified 1,203 genes that overlapped between the DMGs and DEGs related to HCC (Figure 1A). To construct a co-expression network, we chose a soft-thresholding power (β) of 4, resulting in a WGCNA containing the overlapping genes (Figure 1B). The co-expression network formed 12 modules, each consisting of at least 30 genes and represented by different colors (Figure 1C). Notably, the brown module showed a strong association with the HCC phenotype (Figure 1D). Through gene ontology (GO) enrichment analysis, we found 175 genes within the brown module that were associated with immune and oxidative stress biological processes, including modulation of cellular response to oxidative stress, neuron death in response to oxidative stress, activation of immune response, and regulation of immune effector process (Figure 1E).

Construction of HPSM

We performed Cox regression analysis on the methylation-CpG sites of the 175 genes related to oxidative stress and immunity to determine key prognostic methylation-CpG sites. The results revealed that four methylation-CpG sites significantly affected the prognosis of HCC patients: cg14709481, cg09827833, cg13030582, and cg17561435 (Figure 2A). Subsequently, a HPSM risk score was constructed using the following formula: risk score = (-0.45938 × M-value of cg14709481) + (0.120214 × M-value of cg09827833) + (0.15969 × M-value of cg17561435) + (-0.38992 × M-value of cg13030582). Utilizing the median observed risk score, the training dataset (n=186) were divided into two groups: HPSM-high (n=93) as well as HPSM-low (n=93). The HPSM-high group's OS was significantly lower in contrast with that of the HPSM-low group (Figure 2B, $p<0.01$). We evaluated the accuracy of the HPSM prediction model using the AUC, which yielded a value of 0.704 for OS (Figure 2E). The testing dataset (n=185) were divided into HPSM-high (n=98) as well as HPSM-low (n=87) groups. Significant differences in OS rates were observed in the HPSM-high and HPSM-low groups (Figure 2C, $p<0.05$), with an AUC value of 0.638 (Figure 2F). The GSE52018 dataset was used as exterior data to validate the HPSM model's accuracy and reliability, and the survival curve and ROC curve yielded consistent conclusions (Figure 2D, 2G).

Molecular characteristics and immunological characterization of the HPSM subgroups

To explore key signaling pathways in the HPSM subgroups, we performed GSEA on gene sets enriched in the HPSM-high/HPSM-low groups. Results showed that the HPSM-high group was enriched in cell cycle, peroxisome, as well as spliceosome pathways (Figure 3A). On the other hand, the HPSM-low group showed enrichment in metabolic pathways such as drug metabolism cytochrome, threonine metabolism, P450, glycine, serine, porphyrins and chlorophyll metabolism, and retinol metabolism (Figure 3B). Moreover, gene sets associated with good survival of HCC patients were enriched in the HPSM-low group (Figure 3C, 3D). By conducting GSEA focused on immune pathways, we found that 52 pathways related with immune were enriched among the HPSM-low group but not among the HPSM-high group (Figure 3E). Additionally, using ssGSEA, we observed higher levels of tumor-infiltrating immune cell subsets along with immune-associated functions among HPSM-low group in contrast with the HPSM-high group (Figure 3F). Furthermore, the 25 genes with the highest mutation rates were identified among the HPSM subgroup (Figure 3G, 3H). TP53,

TTN, CTNNB1, and MUC16 exhibited mutation rates exceeding 13% in both groups. Notably, TP53 mutations showed the largest difference in mutations between the HPSM subgroups, with a higher prevalence in HPSM-high samples (35%) compared to HPSM-low samples (19%).

Prognostic analysis of HPSM and nomogram development

Univariate and multivariate Cox regression analyses was operated to evaluate the association between HPSM hazard scoring, M staging, T staging, and the prognosis

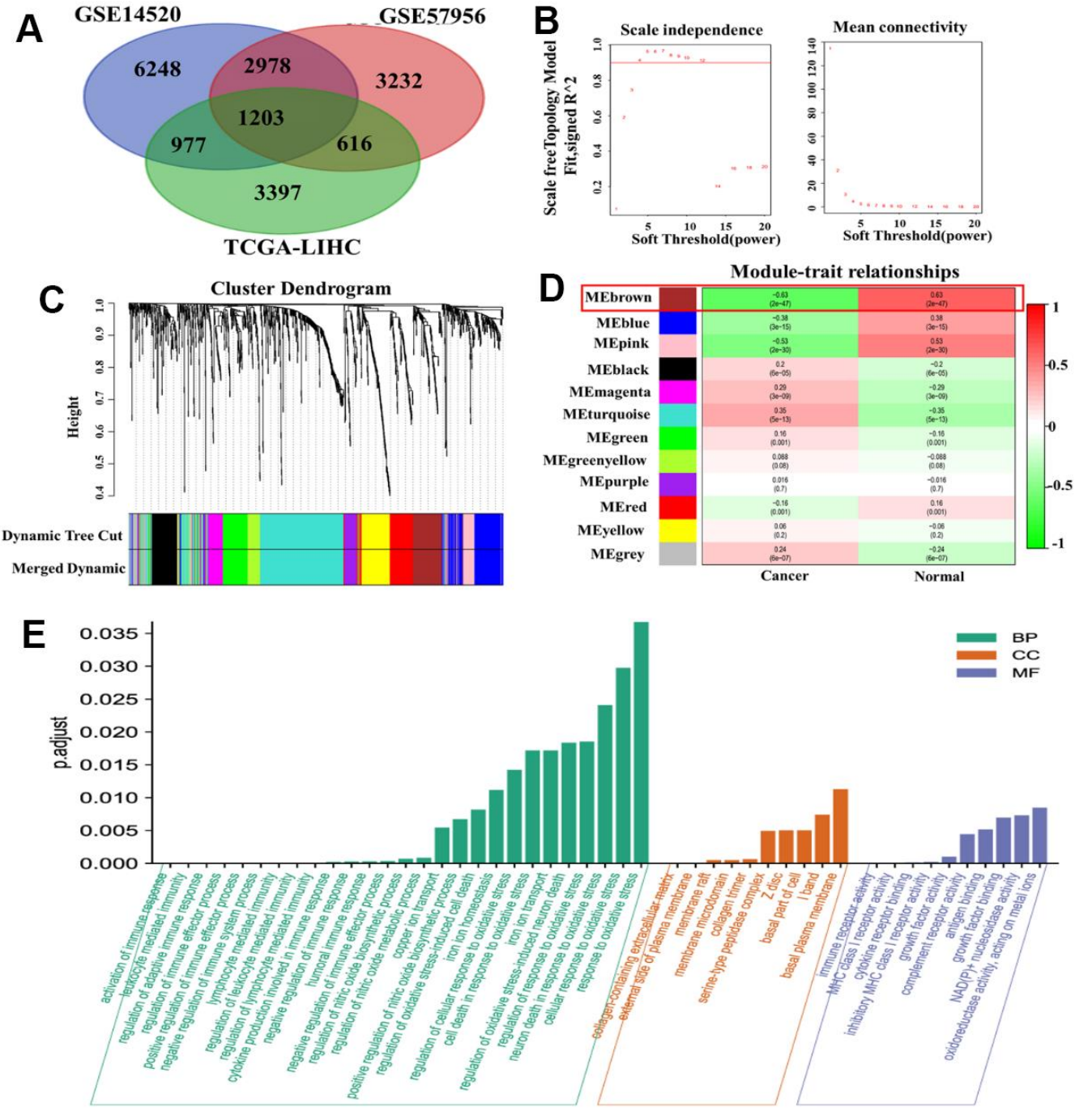

Figure 1. WGCNA of DMGs and DEGs in HCC. (**A**) Identification of overlapping genes between DMGs and DEGs. (**B**) Analysis of the scale-free fit index for different soft threshold powers (β). (**C**) Clustering dendrogram revealing the presence of 12 modules. (**D**) Correlation matrix showing the relationships between these modules in normal and cancer tissues: red indicates positive correlations, while green represents negative correlations. (**E**) GO enrichment analysis of 175 genes associated with oxidative stress and immunity.

of HCC patients (Figure 4A). ROC curve's AUC was calculated as 0.674 for the HPSM hazard scoring (Figure 4B). Based on these results, we developed a nomogram that demonstrated a higher contribution to the model with increasing HPSM risk scores, and lower 1-, 2-, and 3-year survival rates (Figure 4C). The AUCs were found to be 0.721, 0.700, and 0.753 for 1-, 2-, and 3-year OS of HCC patients, respectively (Figure 4D). Additionally, the clinicopathological characteristics of the patients indicated significant correlations between the HPSM groups and multi-nodularity, Cancer of the Liver Italian Program (CLIP) staging, Alpha-fetoprotein (APF), and survival times of HCC patients (Table 1). Therefore, the HPSM risk score may act as an important prognostic indicator for HCC individuals.

Drug sensitivity analysis

A drug sensitivity experiment was conducted to study the relationship between CpG sites' methylation levels in the HPSM and drug sensitivity. It was found that the methylation of cg13030582 was in a negative correlation with sensitivity to nelarabine, carmustine,

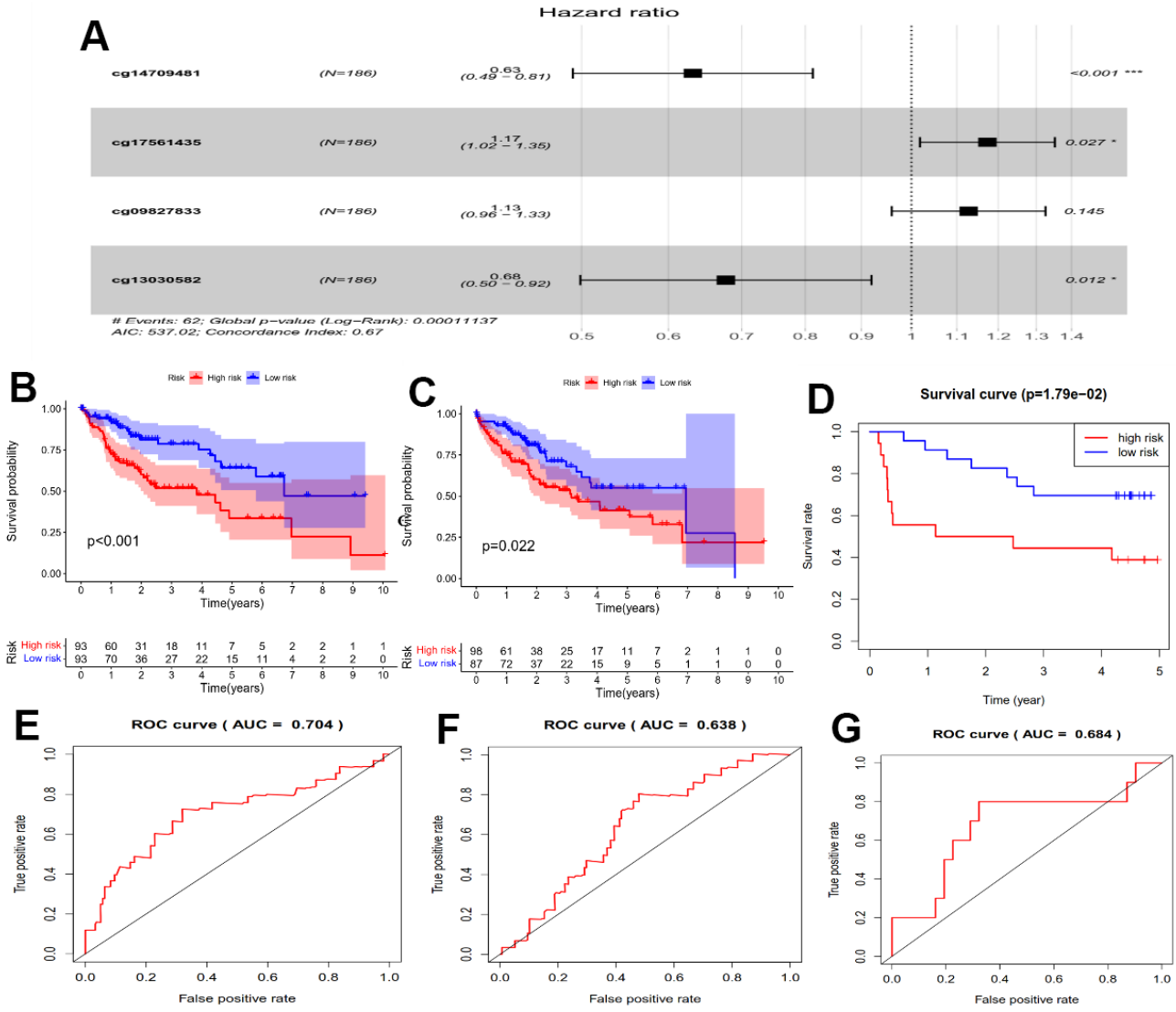

Figure 2. Prognostic analysis of the HPSM subgroups. (**A**) Forest plot displaying the hazard ratios (HRs) for 4 CpGs and OS. (**B**) Kaplan-Meier survival curves for OS comparing HPSM-high group with HPSM-low group within the TCGA training dataset. (**C**) Kaplan-Meier survival curves for OS comparing HPSM-high group with HPSM-low group within the TCGA testing dataset. (**D**) Kaplan-Meier survival curves for OS comparing HPSM-high group with HPSM-low groups within the GSE52018 dataset. (**E**) ROC curves to predict the OS between HPSM groups within the TCGA training dataset. (**F**) ROC curves for OS prediction between HPSM groups within the TCGA testing dataset. (**G**) ROC curves for OS prediction between HPSM groups within the GSE52018 dataset.

bendamustine, melphalan, arsenic trioxide, ifosfamide, etoposide, epirubicin, carboplatin, chlorambucil, and uracil mustard. Methylation levels of cg09827833 were also negatively correlated with sensitivity to isotretinoin, calusterone, fluphenazine, and arsenic trioxide. Furthermore, the methylation level of cg14709481 showed a negative correlation with sensitivity to vemurafenib (Figure 5). These results suggest that the methylation levels of these specific CpG sites in HPSM may be associated with drug sensitivity, providing a clue for further investigation into individualized therapy for HCC patients.

Regulation of BMPER expression by promoter methylation

Among the CpG sites in HPSM, cg17561435 exhibited a greater methylation level among the HPSM-high group compared to HPSM-low group (Figure 6A). The 5' end of the BMPER gene contains a CpG island spanning 1844 bp and consisting of 153 CpG sites. Methylation of the cg17561435 site was found to be negatively correlated with BMPER mRNA expression (Figure 6B). To confirm this regulation, the 19 CpG sites' methylation level among CpG islands using BSP

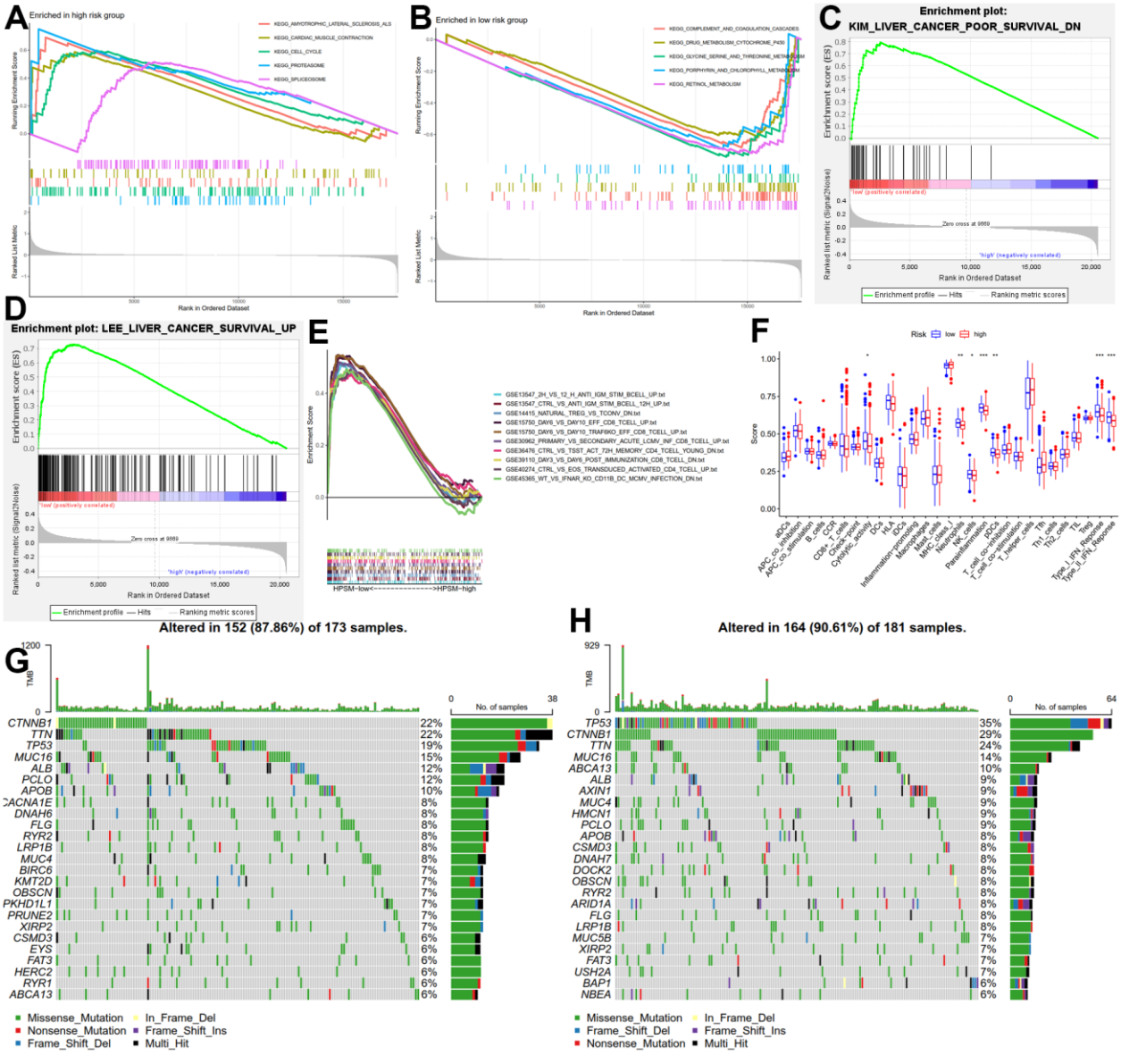

Figure 3. Molecular and immune function analysis among HPSM groups. (**A**) Enriched gene sets among the HPSM-high group. (**B**) Enriched gene sets among the HPSM-low group. (**C**, **D**) GSEA of HPSM subgroups in survival-related gene sets. (**E**) GSEA enrichment analysis of HPSM subgroups in immune-related gene sets. (**F**) Scores of 29 tumor-infiltrating immune cell subsets and immune-related functions. (**G**) TMB analysis in HPSM-low groups. (**H**) TMB analysis in HPSM-high groups.

was analyzed. The results demonstrated a significant reduction in BMPER methylation levels after treatment with 5-aza-dC compared to controls (Figure 6C). Additionally, both qPCR and WB showed increased mRNA / protein levels of BMPER in both cell lines following 5-aza-dC therapy ($p < 0.05$) (Figure 6D, 6E). These findings indicated that BMPER expression could be regulated by promoter methylation.

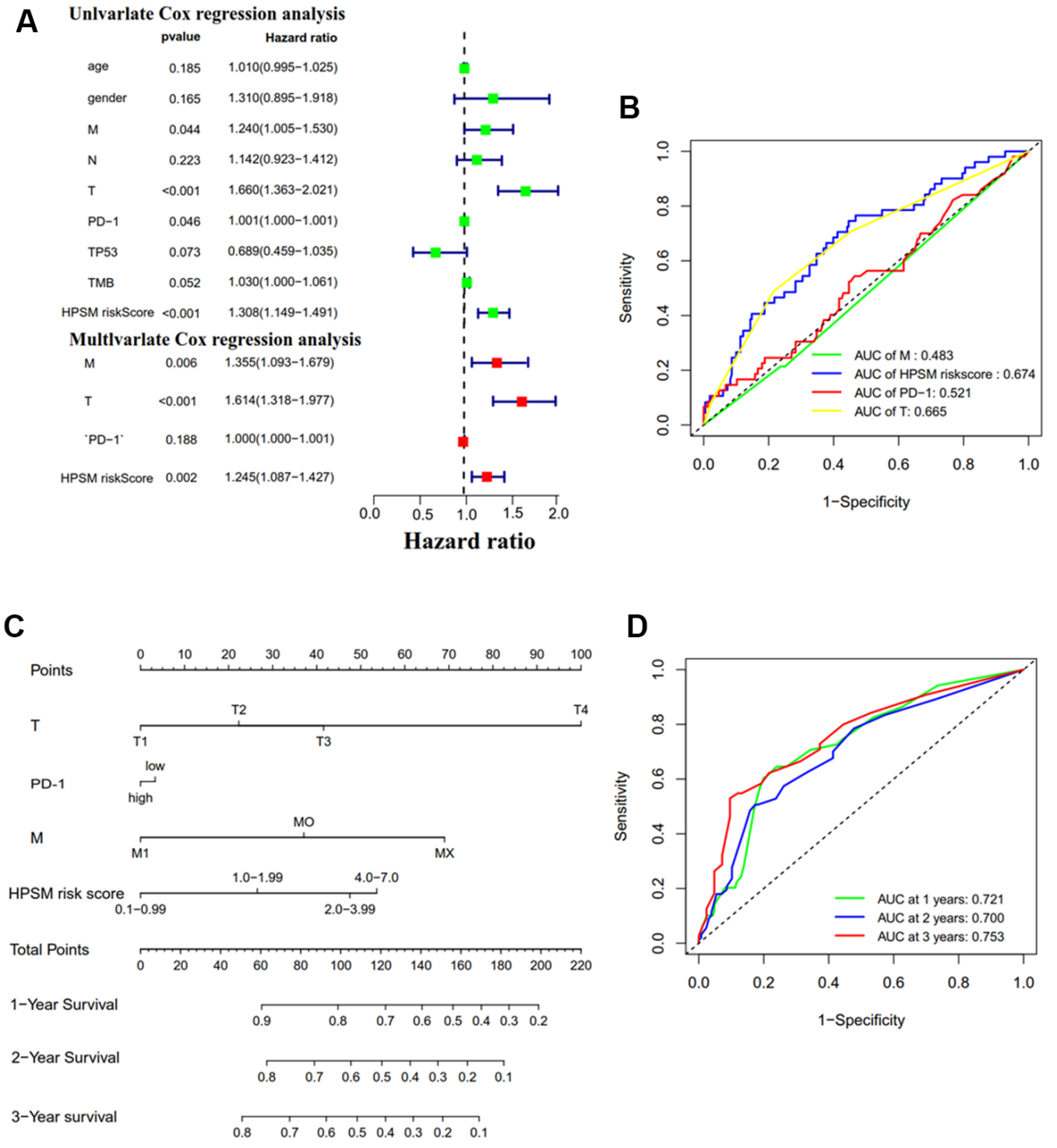

Figure 4. Prognostic analysis of HPSM and nomogram development. (**A**) Univariate and multivariate Cox regression analyses of HPSM risk score as well as prognostic parameters. (**B**) ROC curves of HPSM risk score and prognostic parameters. (**C**) Prognostic nomogram predicting 1-, 2-, and 3-year OS of HCC individuals. (**D**) ROC curves of the prognostic nomogram.

Table 1. Relationship of HPSM risk score with clinicopathological characteristics of HCC.

Clinicopathological parameters	n	HPSM groups		P
		HPSM-high	HPSM-low	
gender				
Male	39	18	21	0.581
Female	2	0	2	
Age				
≤50	26	13	13	0.300
>50	15	5	10	
ALT				
Low	22	8	14	0.200
High	19	10	9	
Main tumor size				
≤3 cm	21	7	14	0.162
>3 cm	20	11	9	
Multinodular				
No	29	10	19	0.018
Yes	12	9	3	
Cirrhosis				
No	5	1	4	0.504
Yes	36	17	19	
TNM staging				
I	15	4	11	0.172
III+II	18	9	9	
BCLC staging				
0+A	22	8	14	0.620
B+C	11	5	6	
CLIP staging				
0+1+2	28	8	20	0.012
3+4+5	5	5	0	
AFP				
≤300 ng/ml	21	4	17	0.001
>300 ng/ml	20	14	6	
survival status				
Alive	23	7	16	0.05
Dead	18	11	7	
survival times				
≤6 months	8	8	0	0.002
>6 months	33	10	23	
recurrence status				
False	13	3	10	0.085
True	27	14	13	
recurrence times				
≤36 months	23	12	11	0.150
>36 months	17	5	12	

Inhibition of HCC cell proliferation by BMPER

To investigate BMPER's biological function in HCC, GSEA enrichment analysis was conducted. We found that cell death in oxidative stress biological process was enriched in the group with low BMPER expression levels (Figure 7A). To further validate these results, we established a BMPER overexpression model in the Hep3B cell line (Figure 7B). As expected, MTT experiments revealed a significant reduction in cell proliferation among the LV-BMPER group in contrast with LV-NC group ($p < 0.05$) (Figure 7C). Moreover,

clone formation assays demonstrated a significant decrease in clone-forming ability in the LV-BMPER group (Figure 7D). These findings confirmed that BMPER overexpression inhibited the proliferation of HCC cells.

DISCUSSION

Algorithms that integrate DNA methylation prognostic markers, oxidative stress, and immune function indicators have shown improved prediction of markers for the prognosis as well as therapeutic targets [23, 24]. In the present study, 175 genes related to oxidative stress and immunity were identified. Subsequently, we con-structed the HPSM consisting of four methylation sites: cg14709481 of HK3, cg09827833 of TEK, cg13030582 of MFAP4, and cg17561435 of BMPER. The TCGA training and testing datasets confirmed a poor prognosis among HCC patients showing a high HPSM risk score, and this finding was also validated in external GEO cohorts. HK3, an isomer of hexokinase responsible for the initial step of glucose metabolism and cell protection against oxidant-induced death, particularly in immune cells [25–27]. Studies have shown that HK3 is associated with immune infiltration; besides it can predict the response to immunotherapy [28]. In our HPSM model, the hypomethylation of cg14709481 in HK3 was significantly associated with a higher HPSM risk score, suggesting that cg14709481 hypomethylation may serve as a poor prognostic factor for HCC patients. TEK, a receptor tyrosine kinase expressed in vascular endothelial cells, exerts its effect on endoplasmic reticulum stress-induced cell death [29]. Monocytes expressing TIE2 not only regulate HCC angiogenesis but also suppress the activation of T cells and promote the expansion of regulatory T cells [30–32]. Consistent with our findings, MFAP4 has been proposed as a molecular marker for HCC diagnosis and prognosis [33]. BMPER binds to BMP and regulates TGF-β/BMP signaling. Previous studies have linked BMPER to lung cancer and ovarian cancer [34, 35], and it has been shown that BMPER expression is controlled by methylation at the transcriptional level. Treatment with 5-aza-dC can reduce BMPER expression in fibroblasts and mitigate invasion and migration of idiopathic pulmonary fibrosis lung fibroblasts [35]. In

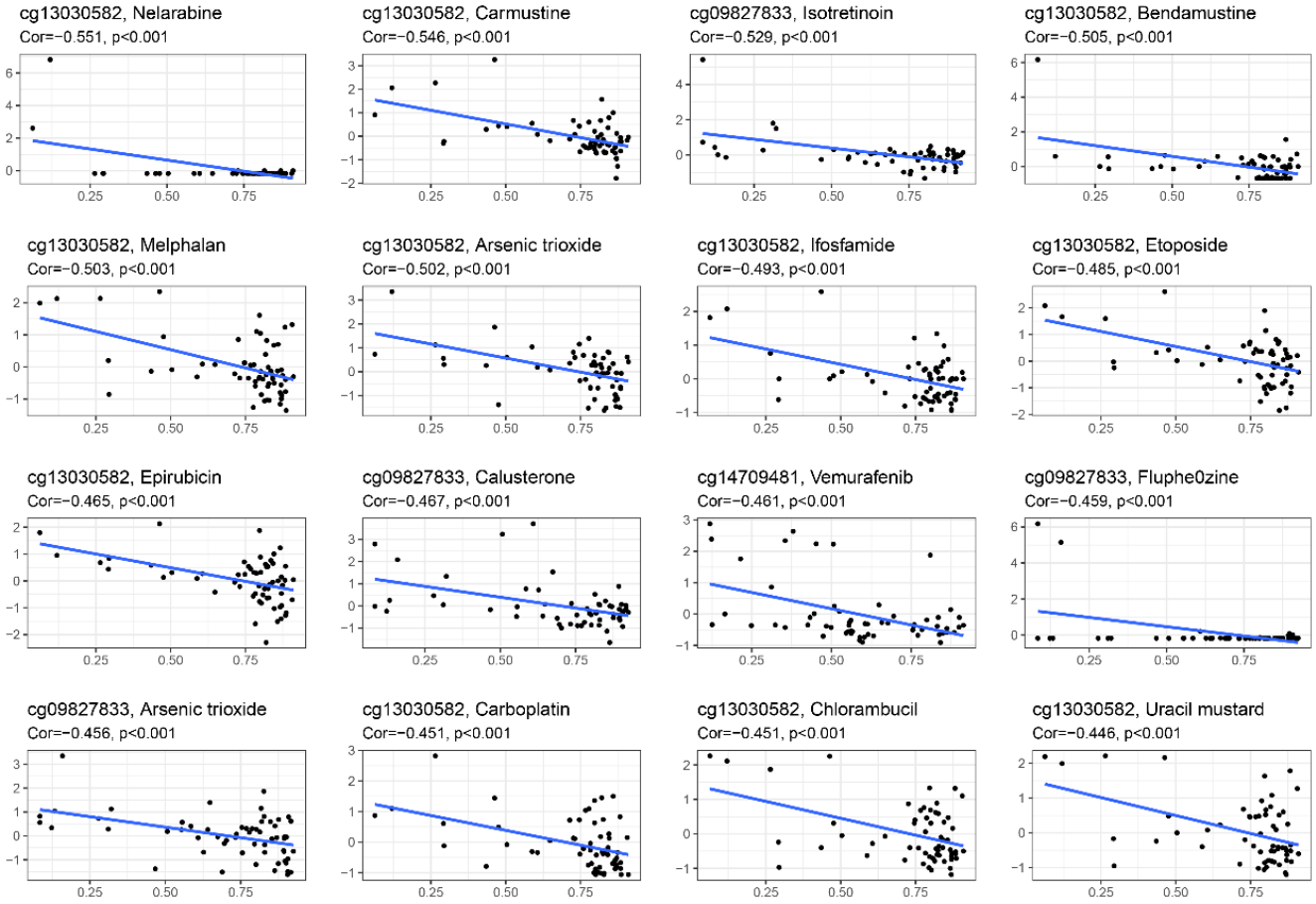

Figure 5. Relationship between methylation levels of CpG sites in the HPSM and FDA drug sensitivity.

our study, we observed a positive correlation between hypermethylation of cg17561435 in BMPER and the HPSM risk score, suggesting that BMPER hypermethylation may be closely associated with poor prognosis in HCC.

Clinical trials have demonstrated that the absence of clinical benefits from cell cycle passage correlates primarily with TP53 mutations [36]. TP53 mutation is associated with more invasive diseases and poorer outcomes [37, 38] in cancer patients, particularly those with HCC [39, 40], TP53 can affect the cell cycle pathway through p53/TGF-β signaling [41]. Interestingly, we found enrichment of the cell cycle pathway in the HPSM-high group, where TP53 mutations were more prevalent and the prognosis was worse compared to the HPSM-low group. These results suggest that TP53 mutations may influence the cell cycle pathway and contribute to a poorer prognosis in the HPSM-high group.

Two gene sets related to good prognosis in HCC patients were enriched in the HPSM-low group, indicating better OS for HPSM-low group in contrast with HPSM-high group, consistent with prognostic prediction on the basis of the HPSM risk score. Higher levels of tumor-infiltrating immune cells have been demonstrated to be generally linked to a better prognosis [42–44]. Neutrophils, natural killer (NK) cells, plasma cytotoxic dendritic cells (pCDs), and type I and II interferon (IFN) reactions were obviously higher among the HPSM-low group in contrast with HPSM-high group. Studies have shown that type II immune interferons (IFNs) are in a close association

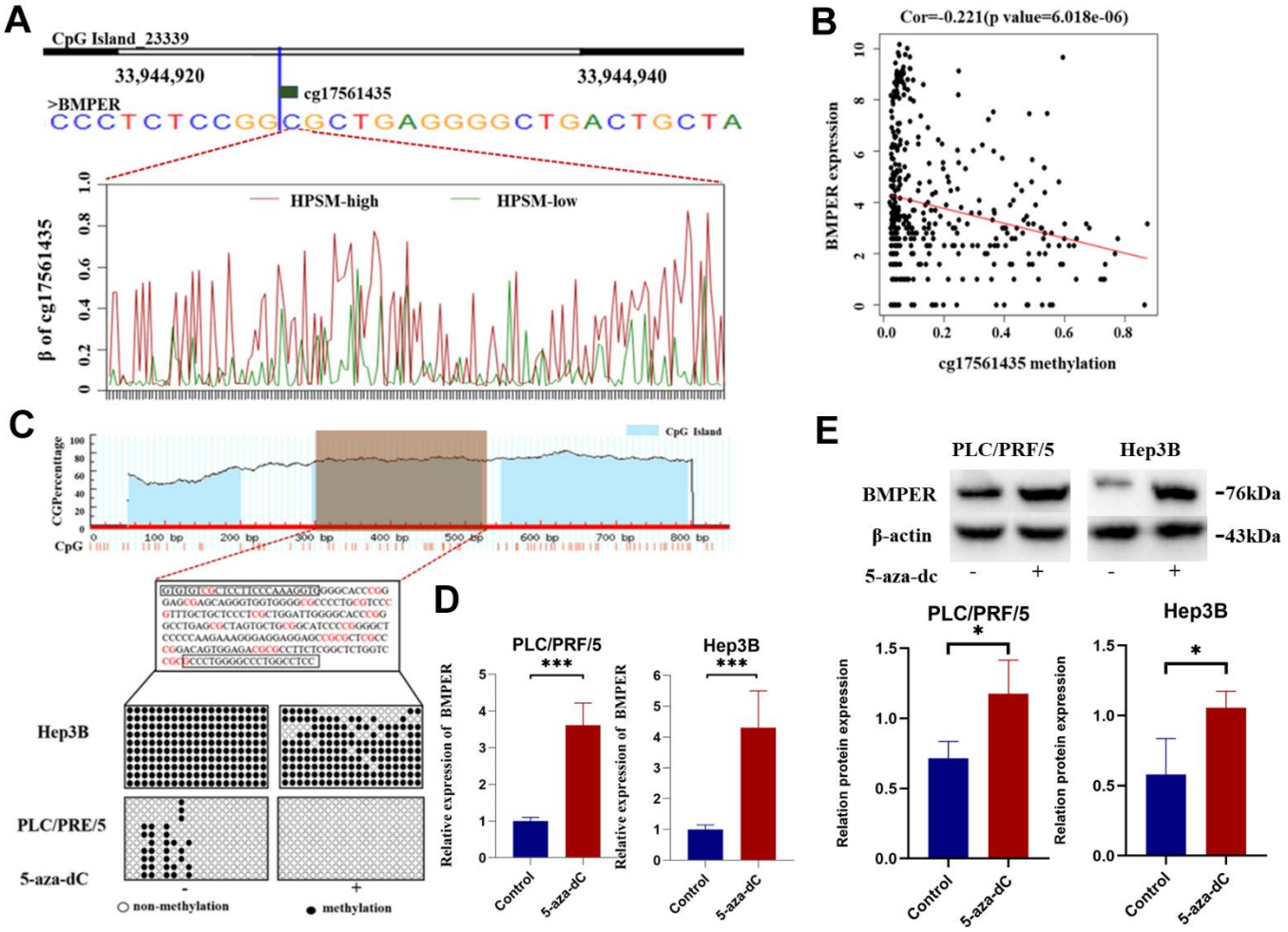

Figure 6. Regulation of BMPER expression by promoter methylation. (**A**) Methylation level of cg17561435 in different HPSM subgroups. (**B**) Negative correlation between BMPER mRNA expression and cg17561453 methylation levels. (**C**) Prediction of CpG islands in the BMPER promoter using the MethPrimer website, and detection of BMPER promoter methylation status using bisulfite sequencing PCR (BSP). (**D**) Quantification of BMPER mRNA expression levels after 5-aza-dC treatment using qPCR (***$p < 0.01$). (**E**) Detection of BMPER protein expression levels after 5-aza-dC treatment using western blotting.

with favorable clinical outcomes within various cancer types [45–47]. which is consistent with our findings. Furthermore, we observed enrichment of the amino acid metabolism pathway among the HPSM-low group. A recent study reported that amino acid metabolism enhances the immune response against tumors [48]. Serine, in particular, is an essential nutrient for T cell responses and a critical mediator of the anti-tumor immune response [49–51]. Taken together, our results suggest that the HPSM-low group elicits a more robust tumor immune response than the HPSM-high group, leading to better OS.

Cox regression analyses revealed that HPSM risk scoring, M staging, and T staging are independent prognostic factors for HCC. HPSM risk score's AUC (0.674) was higher compared to that of T stage (0.665) and M stage (0.483), indicating that the HPSM risk score is a more accurate prognostic factor. Thus, we developed a prognostic nomogram model by integrating traditional clinical features with the HPSM risk score. This score significantly contributes to the predictive ability of the entire nomogram, showing robust performance (AUC≥0.7). Our study suggests that the HPSM risk score is a valuable independent prognostic indicator. Patients with multinodular HCC accompanied by vascular invasion and microvascular invasion have more invasive tumors and a higher rate of recurrence, leading to poor prognosis [52]. The CLIP staging system provides more accurate prognostic information than the Child-Pugh and Okuda classifications, with higher scores indicating worse prognosis in HCC patients [53–55]. Numerous studies have established a strong association between higher levels of AFP in the blood and worse prognosis and increased risk of recurrence in HCC patients [56–58]. In this study, we found that the HPSM risk score correlates with these clinicopathological characteristics and the survival time of HCC patients, highlighting its significant role in the course of HCC. The HPSM risk score may be an important biomarker for estimating the risk of HCC recurrence, progression, further facilitating the selection of treatment options.

The CpG sites of HPSM are closely related to FDA-approved drugs. Previous studies have demonstrated that isotretinoin, fluphenazine, and arsenic trioxide induce oxidative stress as part of disease treatment

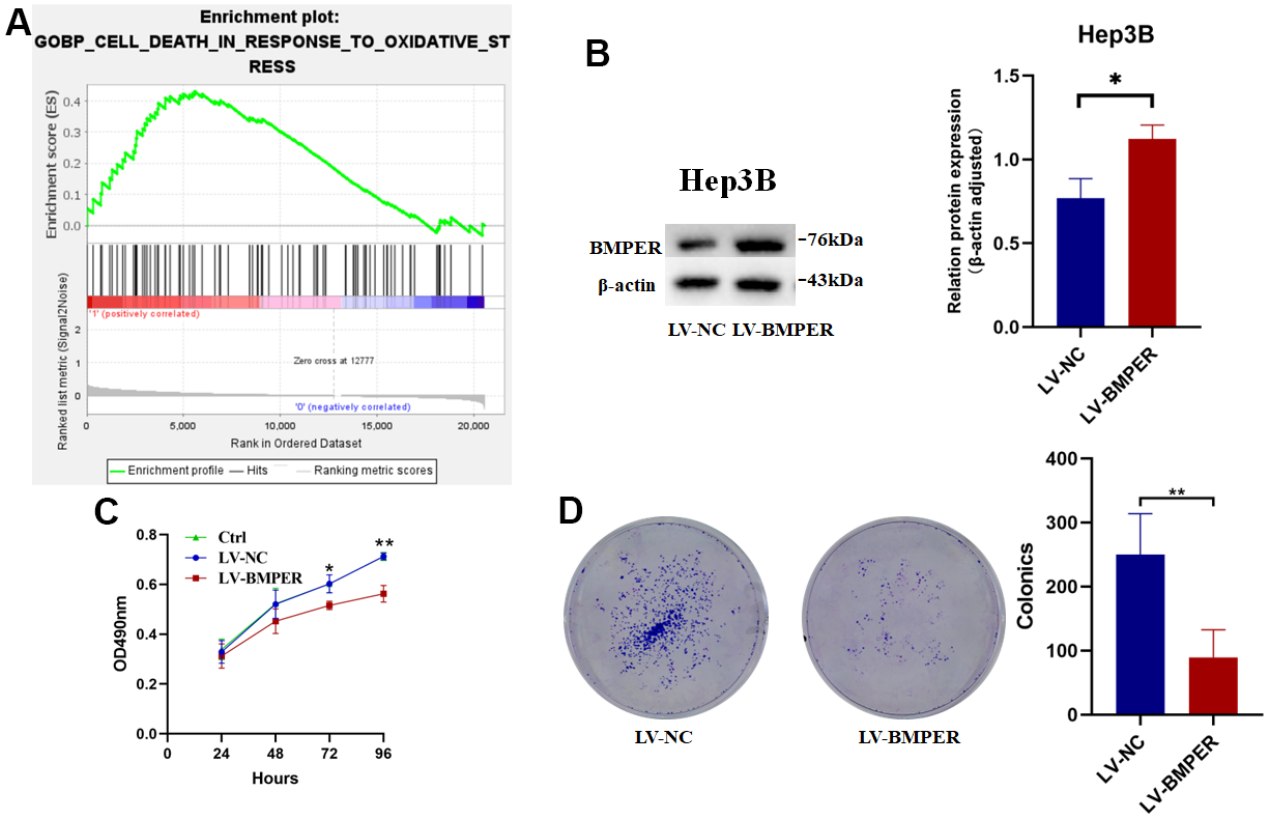

Figure 7. Inhibition of HCC cell proliferation by BMPER overexpression. (**A**) GO biological process pathway enrichment analysis using GSEA. (**B**) Confirmation of BMPER overexpression in Hep3B cell line using western blotting. (**C**) Effects of BMPER overexpression on cell proliferation assessed by MTT assays. (**D**) Clonal formation assays comparing the LV-NC and LV-BMPER groups.

[59–62]. Interestingly, the methylation level of cg09827833is negatively correlated with isotretinoin, arsenic trioxide, and fluphenazine. Methylation of cg14709481 is negatively associated with the sensitivity of the BRAF inhibitor vemurafenib. Several studies have highlighted the immunomodulatory effects of anti-tumor drugs [63]. BRAF inhibitors, for example, increase levels of immunostimulatory cytokines, reduce immunosuppressive cytokines, and decrease T cell infiltration and activity in tumors through interference with the MAPK signaling pathway [64]. Combining BRAF inhibitors with immune checkpoint inhibitors may lead to better tumor suppression. The methylation level of cg13030582 is negatively correlated with immunomodulatory inhibitors such as isotretinoin, DNA synthesis inhibitors (etoposide, epirubicin, carbolatin), and DNA alkylating agent carmustine. Isotretinoin induces apoptosis of liver cancer cells by reducing the activities of superoxide dismutase (SOD), peroxidase (POD), and glutathione (G-SH) [65]. Etoposide mediates reactive oxygen species (ROS) production and induces necrosis in HK-2 cells through a p53-mediated anti-apoptotic pathway [66]. Carbolatin promotes LSCC cell apoptosis through the induction of oxidative stress and ROS production [67]. Carmustine induces ROS production and promotes neurotoxicity [68]. The combination of tumor immunotherapy and oxidative stress represents a potentially effective strategy for tumor treatment, enhancing antitumor activity mediated by immune cells and inducing oxidative stress in tumor cells. HPSM may serve as a potential target for oxidative stress and immunomodulators or an effective marker for predicting drug sensitivity.

In our study, the methylation level of cg17561435 was demonstrated to be positively linked to the HPSM risk score. Furthermore, we confirmed that BMPER expression was associated with cell death in response to oxidative stress, and BMPER overexpression inhibited the proliferation of HCC cells. Whether the role of BMPER in inhibiting tumor cell proliferation is caused by oxidative stress needs further verification. These results provided evidence for the crucial function of BMPER in HCC progression, necessitating further investigation.

CONCLUSIONS

In conclusion, the HPSM, constructed based on four CpG sites, serves as a valuable independent prognostic factor. Additionally, the HPSM risk score could predict the efficacy of immunotherapy in HCC patients. Moreover, the CpG sites were associated with drug sensitivity, providing guidance for individualized treatment approaches for HCC.

AUTHOR CONTRIBUTIONS

ZJM, JTG and GQY designed and directed the research. CMH and ZHG contributed to the analysis and interpretation of data and wrote the main manuscript text; CMH, ZHG, and HZ performed the experiments and analyzed results. All authors read and approved the final manuscript.

CONFLICTS OF INTEREST

The authors declare that they have no conflicts of interest.

FUNDING

This work was supported by the National Natural Science Foundation of China (32060159), and Guangxi Natural Science Foundation (2020GXNSFAA159110).

REFERENCES

1. Lee JH, Suh JH, Choi SY, Kang HJ, Lee HH, Ye BJ, Lee GR, Jung SW, Kim CJ, Lee-Kwon W, Park J, Myung K, Park NH, Kwon HM. Tonicity-responsive enhancer-binding protein promotes hepatocellular carcinogenesis, recurrence and metastasis. Gut. 2019; 68:347–58. https://doi.org/10.1136/gutjnl-2017-315348 PMID:29420225

2. Fu Y, Silverstein S, McCutcheon JN, Dyba M, Nath RG, Aggarwal M, Coia H, Bai A, Pan J, Jiang J, Kallakury B, Wang H, Zhang YW, et al. An endogenous DNA adduct as a prognostic biomarker for hepatocarcinogenesis and its prevention by Theaphenon E in mice. Hepatology. 2018; 67:159–70. https://doi.org/10.1002/hep.29380 PMID:28718980

3. Muriel P. Role of free radicals in liver diseases. Hepatol Int. 2009; 3:526–36. https://doi.org/10.1007/s12072-009-9158-6 PMID:19941170

4. Lim SO, Gu JM, Kim MS, Kim HS, Park YN, Park CK, Cho JW, Park YM, Jung G. Epigenetic changes induced by reactive oxygen species in hepatocellular carcinoma: methylation of the E-cadherin promoter. Gastroenterology. 2008; 135:2128–40. https://doi.org/10.1053/j.gastro.2008.07.027 PMID:18801366

5. Esteller M. Cancer epigenomics: DNA methylomes and histone-modification maps. Nat Rev Genet. 2007; 8:286–98. https://doi.org/10.1038/nrg2005 PMID:17339880

6. Jones PA, Baylin SB. The fundamental role of epigenetic events in cancer. Nat Rev Genet. 2002; 3:415–28.

https://doi.org/10.1038/nrg816
PMID:12042769

7. Tao Y, Kang B, Petkovich DA, Bhandari YR, In J, Stein-O'Brien G, Kong X, Xie W, Zachos N, Maegawa S, Vaidya H, Brown S, Chiu Yen RW, et al. Aging-like Spontaneous Epigenetic Silencing Facilitates Wnt Activation, Stemness, and BrafV600E-Induced Tumorigenesis. Cancer Cell. 2019; 35:315–28.e6. https://doi.org/10.1016/j.ccell.2019.01.005 PMID:30753828

8. Xia L, Huang W, Bellani M, Seidman MM, Wu K, Fan D, Nie Y, Cai Y, Zhang YW, Yu LR, Li H, Zahnow CA, Xie W, et al. CHD4 Has Oncogenic Functions in Initiating and Maintaining Epigenetic Suppression of Multiple Tumor Suppressor Genes. Cancer Cell. 2017; 31:653–68.e7. https://doi.org/10.1016/j.ccell.2017.04.005 PMID:28486105

9. Ehrhart F, Roozen S, Verbeek J, Koek G, Kok G, van Kranen H, Evelo CT, Curfs LM. Review and gap analysis: molecular pathways leading to fetal alcohol spectrum disorders. Mol Psychiatry. 2019; 24:10–7. https://doi.org/10.1038/s41380-018-0095-4 PMID:29892052

10. Qian H, Chao X, Williams J, Fulte S, Li T, Yang L, Ding WX. Autophagy in liver diseases: A review. Mol Aspects Med. 2021; 82:100973. https://doi.org/10.1016/j.mam.2021.100973 PMID:34120768

11. Zhang P, Chen Z, Kuang H, Liu T, Zhu J, Zhou L, Wang Q, Xiong X, Meng Z, Qiu X, Jacks R, Liu L, Li S, et al. Neuregulin 4 suppresses NASH-HCC development by restraining tumor-prone liver microenvironment. Cell Metab. 2022; 34:1359–76.e7. https://doi.org/10.1016/j.cmet.2022.07.010 PMID:35973424

12. Mo Z, Zheng S, Lv Z, Zhuang Y, Lan X, Wang F, Lu X, Zhao Y, Zhou S. Senescence marker protein 30 (SMP30) serves as a potential prognostic indicator in hepatocellular carcinoma. Sci Rep. 2016; 6:39376. https://doi.org/10.1038/srep39376 PMID:27991558

13. Tang H, You T, Sun Z, Bai C. A Comprehensive Prognostic Analysis of POLD1 in Hepatocellular Carcinoma. BMC Cancer. 2022; 22:197. https://doi.org/10.1186/s12885-022-09284-y PMID:35189839

14. Zeng Z, Jiang X, Pan Z, Zhou R, Lin Z, Tang Y, Cui Y, Zhang E, Cao Z. Highly expressed centromere protein L indicates adverse survival and associates with immune infiltration in hepatocellular carcinoma. Aging (Albany NY). 2021; 13:22802–29. https://doi.org/10.18632/aging.203574 PMID:34607313

15. de Vos L, Grünwald I, Bawden EG, Dietrich J, Scheckenbach K, Wiek C, Zarbl R, Bootz F, Landsberg J, Dietrich D. The landscape of CD28, CD80, CD86, CTLA4, and ICOS DNA methylation in head and neck squamous cell carcinomas. Epigenetics. 2020; 15:1195–212. https://doi.org/10.1080/15592294.2020.1754675 PMID:32281488

16. Barbie DA, Tamayo P, Boehm JS, Kim SY, Moody SE, Dunn IF, Schinzel AC, Sandy P, Meylan E, Scholl C, Fröhling S, Chan EM, Sos ML, et al. Systematic RNA interference reveals that oncogenic KRAS-driven cancers require TBK1. Nature. 2009; 462:108–12. https://doi.org/10.1038/nature08460 PMID:19847166

17. Aryee MJ, Jaffe AE, Corrada-Bravo H, Ladd-Acosta C, Feinberg AP, Hansen KD, Irizarry RA. Minfi: a flexible and comprehensive Bioconductor package for the analysis of Infinium DNA methylation microarrays. Bioinformatics. 2014; 30:1363–9. https://doi.org/10.1093/bioinformatics/btu049 PMID:24478339

18. Jin Y, Wang Z, He D, Zhu Y, Chen X, Cao K. Identification of novel subtypes based on ssGSEA in immune-related prognostic signature for tongue squamous cell carcinoma. Cancer Med. 2021; 10:8693–707. https://doi.org/10.1002/cam4.4341 PMID:34668665

19. Wang W, Lu Z, Wang M, Liu Z, Wu B, Yang C, Huan H, Gong P. The cuproptosis-related signature associated with the tumor environment and prognosis of patients with glioma. Front Immunol. 2022; 13:998236. https://doi.org/10.3389/fimmu.2022.998236 PMID:36110851

20. Tamura R. Current Understanding of Neurofibromatosis Type 1, 2, and Schwannomatosis. Int J Mol Sci. 2021; 22:5850. https://doi.org/10.3390/ijms22115850 PMID:34072574

21. Janjigian YY, Shitara K, Moehler M, Garrido M, Salman P, Shen L, Wyrwicz L, Yamaguchi K, Skoczylas T, Campos Bragagnoli A, Liu T, Schenker M, Yanez P, et al. First-line nivolumab plus chemotherapy versus chemotherapy alone for advanced gastric, gastro-oesophageal junction, and oesophageal adenocarcinoma (CheckMate 649): a randomised, open-label, phase 3 trial. Lancet. 2021; 398:27–40. https://doi.org/10.1016/S0140-6736(21)00797-2 PMID:34102137

22. Lungu C, Pinter S, Broche J, Rathert P, Jeltsch A. Modular fluorescence complementation sensors for live cell detection of epigenetic signals at endogenous genomic sites. Nat Commun. 2017; 8:649. https://doi.org/10.1038/s41467-017-00457-z PMID:28935858

23. Xie J, Chen L, Sun Q, Li H, Wei W, Wu D, Hu Y, Zhu Z, Shi J, Wang M. An immune subtype-related prognostic signature of hepatocellular carcinoma based on single-cell sequencing analysis. Aging (Albany NY). 2022; 14:3276–92. https://doi.org/10.18632/aging.204012 PMID:35413690

24. Qiu Y, Li H, Xie J, Qiao X, Wu J. Identification of ABCC5 Among ATP-Binding Cassette Transporter Family as a New Biomarker for Hepatocellular Carcinoma Based on Bioinformatics Analysis. Int J Gen Med. 2021; 14:7235–46. https://doi.org/10.2147/IJGM.S333904 PMID:34737618

25. van Diepen A, Brand HK, de Waal L, Bijl M, Jong VL, Kuiken T, van Amerongen G, van den Ham HJ, Eijkemans MJ, Osterhaus AD, Hermans PW, Andeweg AC. Host proteome correlates of vaccine-mediated enhanced disease in a mouse model of respiratory syncytial virus infection. J Virol. 2015; 89:5022–31. https://doi.org/10.1128/JVI.03630-14 PMID:25694607

26. Federzoni EA, Valk PJ, Torbett BE, Haferlach T, Löwenberg B, Fey MF, Tschan MP. PU.1 is linking the glycolytic enzyme HK3 in neutrophil differentiation and survival of APL cells. Blood. 2012; 119:4963–70. https://doi.org/10.1182/blood-2011-09-378117 PMID:22498738

27. Jun HS, Weinstein DA, Lee YM, Mansfield BC, Chou JY. Molecular mechanisms of neutrophil dysfunction in glycogen storage disease type Ib. Blood. 2014; 123:2843–53. https://doi.org/10.1182/blood-2013-05-502435 PMID:24565827

28. Tuo Z, Zheng X, Zong Y, Li J, Zou C, Lv Y, Liu J. HK3 is correlated with immune infiltrates and predicts response to immunotherapy in non-small cell lung cancer. Clin Transl Med. 2020; 10:319–30. https://doi.org/10.1002/ctm2.6 PMID:32508023

29. Hosoi T, Tamubo T, Horie N, Okuma Y, Nomura Y, Ozawa K. TEK/Tie2 is a novel gene involved in endoplasmic reticulum stress. J Pharmacol Sci. 2010; 114:230–3. https://doi.org/10.1254/jphs.10082sc PMID:20938104

30. Coffelt SB, Chen YY, Muthana M, Welford AF, Tal AO, Scholz A, Plate KH, Reiss Y, Murdoch C, De Palma M, Lewis CE. Angiopoietin 2 stimulates TIE2-expressing monocytes to suppress T cell activation and to promote regulatory T cell expansion. J Immunol. 2011; 186:4183–90. https://doi.org/10.4049/jimmunol.1002802 PMID:21368233

31. Matsubara T, Kanto T, Kuroda S, Yoshio S, Higashitani K, Kakita N, Miyazaki M, Sakakibara M, Hiramatsu N, Kasahara A, Tomimaru Y, Tomokuni A, Nagano H, et al. TIE2-expressing monocytes as a diagnostic marker for hepatocellular carcinoma correlates with angiogenesis. Hepatology. 2013; 57:1416–25. https://doi.org/10.1002/hep.25965 PMID:22815256

32. Coffelt SB, Tal AO, Scholz A, De Palma M, Patel S, Urbich C, Biswas SK, Murdoch C, Plate KH, Reiss Y, Lewis CE. Angiopoietin-2 regulates gene expression in TIE2-expressing monocytes and augments their inherent proangiogenic functions. Cancer Res. 2010; 70:5270–80. https://doi.org/10.1158/0008-5472.CAN-10-0012 PMID:20530679

33. Li J, Wang J, Liu Z, Guo H, Wei X, Wei Q, Zheng S, Xu X. Tumor-suppressive role of microfibrillar associated protein 4 and its clinical significance as prognostic factor and diagnostic biomarker in hepatocellular carcinoma. J Cancer Res Ther. 2022; 18:1919–25. https://doi.org/10.4103/jcrt.jcrt_693_22 PMID:36647950

34. Huan C, Yang T, Liang J, Xie T, Cheng L, Liu N, Kurkciyan A, Monterrosa Mena J, Wang C, Dai H, Noble PW, Jiang D. Methylation-mediated BMPER expression in fibroblast activation *in vitro* and lung fibrosis in mice *in vivo*. Sci Rep. 2015; 5:14910. https://doi.org/10.1038/srep14910 PMID:26442443

35. Xi Y, Nie X, Wang J, Gao L, Lin B. Overexpression of BMPER in Ovarian Cancer and the Mechanism by which It Promotes Malignant Biological Behavior in Tumor Cells. Biomed Res Int. 2020; 2020:3607436. https://doi.org/10.1155/2020/3607436 PMID:32309430

36. Olivier M, Langerød A, Carrieri P, Bergh J, Klaar S, Eyfjord J, Theillet C, Rodriguez C, Lidereau R, Bièche I, Varley J, Bignon Y, Uhrhammer N, et al. The clinical value of somatic TP53 gene mutations in 1,794 patients with breast cancer. Clin Cancer Res. 2006; 12:1157–67. https://doi.org/10.1158/1078-0432.CCR-05-1029 PMID:16489069

37. Vousden KH, Prives C. P53 and prognosis: new insights and further complexity. Cell. 2005; 120:7–10. https://doi.org/10.1016/j.cell.2004.12.027 PMID:15652475

38. Chaudhary K, Poirion OB, Lu L, Garmire LX. Deep Learning-Based Multi-Omics Integration Robustly Predicts Survival in Liver Cancer. Clin Cancer Res. 2018; 24:1248–59. https://doi.org/10.1158/1078-0432.CCR-17-0853 PMID:28982688

39. Lee JS. The mutational landscape of hepatocellular carcinoma. Clin Mol Hepatol. 2015; 21:220–9. https://doi.org/10.3350/cmh.2015.21.3.220 PMID:26523267

40. Llovet JM, Castet F, Heikenwalder M, Maini MK, Mazzaferro V, Pinato DJ, Pikarsky E, Zhu AX, Finn RS. Immunotherapies for hepatocellular carcinoma. Nat Rev Clin Oncol. 2022; 19:151–72. https://doi.org/10.1038/s41571-021-00573-2 PMID:34764464

41. Chen Y, Li ZY, Zhou GQ, Sun Y. An Immune-Related Gene Prognostic Index for Head and Neck Squamous Cell Carcinoma. Clin Cancer Res. 2021; 27:330–41. https://doi.org/10.1158/1078-0432.CCR-20-2166 PMID:33097495

42. Fridman WH, Zitvogel L, Sautès-Fridman C, Kroemer G. The immune contexture in cancer prognosis and treatment. Nat Rev Clin Oncol. 2017; 14:717–34. https://doi.org/10.1038/nrclinonc.2017.101 PMID:28741618

43. Wang S, Zhang Q, Yu C, Cao Y, Zuo Y, Yang L. Immune cell infiltration-based signature for prognosis and immunogenomic analysis in breast cancer. Brief Bioinform. 2021; 22:2020–31. https://doi.org/10.1093/bib/bbaa026 PMID:32141494

44. Zhang J, Wang J, Qian Z, Han Y. CCR5 is Associated With Immune Cell Infiltration and Prognosis of Lung Cancer. J Thorac Oncol. 2019; 14:e102–3. https://doi.org/10.1016/j.jtho.2018.12.037 PMID:31027743

45. Shankaran V, Ikeda H, Bruce AT, White JM, Swanson PE, Old LJ, Schreiber RD. IFNgamma and lymphocytes prevent primary tumour development and shape tumour immunogenicity. Nature. 2001; 410:1107–11. https://doi.org/10.1038/35074122 PMID:11323675

46. Seresini S, Origoni M, Lillo F, Caputo L, Paganoni AM, Vantini S, Longhi R, Taccagni G, Ferrari A, Doglioni C, Secchi P, Protti MP. IFN-gamma produced by human papilloma virus-18 E6-specific CD4+ T cells predicts the clinical outcome after surgery in patients with high-grade cervical lesions. J Immunol. 2007; 179:7176–83. https://doi.org/10.4049/jimmunol.179.10.7176 PMID:17982110

47. Fridman WH, Pagès F, Sautès-Fridman C, Galon J. The immune contexture in human tumours: impact on clinical outcome. Nat Rev Cancer. 2012; 12:298–306. https://doi.org/10.1038/nrc3245 PMID:22419253

48. Geiger R, Rieckmann JC, Wolf T, Basso C, Feng Y, Fuhrer T, Kogadeeva M, Picotti P, Meissner F, Mann M, Zamboni N, Sallusto F, Lanzavecchia A. L-Arginine Modulates T Cell Metabolism and Enhances Survival and Anti-tumor Activity. Cell. 2016; 167:829–42.e13. https://doi.org/10.1016/j.cell.2016.09.031 PMID:27745970

49. Ma EH, Bantug G, Griss T, Condotta S, Johnson RM, Samborska B, Mainolfi N, Suri V, Guak H, Balmer ML, Verway MJ, Raissi TC, Tsui H, et al. Serine Is an Essential Metabolite for Effector T Cell Expansion. Cell Metab. 2017; 25:345–57. https://doi.org/10.1016/j.cmet.2016.12.011 PMID:28111214

50. Srivastava MK, Sinha P, Clements VK, Rodriguez P, Ostrand-Rosenberg S. Myeloid-derived suppressor cells inhibit T-cell activation by depleting cystine and cysteine. Cancer Res. 2010; 70:68–77. https://doi.org/10.1158/0008-5472.CAN-09-2587 PMID:20028852

51. Frumento G, Rotondo R, Tonetti M, Damonte G, Benatti U, Ferrara GB. Tryptophan-derived catabolites are responsible for inhibition of T and natural killer cell proliferation induced by indoleamine 2,3-dioxygenase. J Exp Med. 2002; 196:459–68. https://doi.org/10.1084/jem.20020121 PMID:12186838

52. Hung HH, Lei HJ, Chau GY, Su CW, Hsia CY, Kao WY, Lui WY, Wu WC, Lin HC, Wu JC. Milan criteria, multi-nodularity, and microvascular invasion predict the recurrence patterns of hepatocellular carcinoma after resection. J Gastrointest Surg. 2013; 17:702–11. https://doi.org/10.1007/s11605-012-2087-z PMID:23225107

53. Duseja A. Staging of hepatocellular carcinoma. J Clin Exp Hepatol. 2014 (Suppl 3); 4:S74–9. https://doi.org/10.1016/j.jceh.2014.03.045 PMID:25755615

54. Prospective validation of the CLIP score: a new prognostic system for patients with cirrhosis and hepatocellular carcinoma. The Cancer of the Liver Italian Program (CLIP) Investigators. Hepatology. 2000; 31:840–5. https://doi.org/10.1053/he.2000.5628 PMID:10733537

55. A new prognostic system for hepatocellular carcinoma: a retrospective study of 435 patients: the Cancer of the Liver Italian Program (CLIP) investigators. Hepatology. 1998; 28:751–5. https://doi.org/10.1002/hep.510280322 PMID:9731568

56. Witjes CD, Polak WG, Verhoef C, Eskens FA, Dwarkasing RS, Verheij J, de Man RA, Ijzermans JN. Increased alpha-fetoprotein serum level is predictive for survival and recurrence of hepatocellular

carcinoma in non-cirrhotic livers. Dig Surg. 2012; 29:522–8.
https://doi.org/10.1159/000348669 PMID:23548745

57. Silva J, Berger N, Gamblin TC. Prognostic significance of baseline alpha-fetoprotein in hepatocellular carcinoma: systematic review and meta-analysis. HPB. 2017; 19:S124.
https://doi.org/10.1016/j.hpb.2017.02.276

58. Kelley RK, Meyer T, Rimassa L, Merle P, Park JW, Yau T, Chan SL, Blanc JF, Tam VC, Tran A, Dadduzio V, Markby DW, Kaldate R, et al. Serum Alpha-fetoprotein Levels and Clinical Outcomes in the Phase III CELESTIAL Study of Cabozantinib versus Placebo in Patients with Advanced Hepatocellular Carcinoma. Clin Cancer Res. 2020; 26:4795–804.
https://doi.org/10.1158/1078-0432.CCR-19-3884
PMID:32636319

59. Di Marcantonio D, Martinez E, Sidoli S, Vadaketh J, Nieborowska-Skorska M, Gupta A, Meadows JM, Ferraro F, Masselli E, Challen GA, Milsom MD, Scholl C, Fröhling S, et al. Protein Kinase C Epsilon Is a Key Regulator of Mitochondrial Redox Homeostasis in Acute Myeloid Leukemia. Clin Cancer Res. 2018; 24:608–18.
https://doi.org/10.1158/1078-0432.CCR-17-2684
PMID:29127121

60. Duarte D, Vale N. Antipsychotic Drug Fluphenazine against Human Cancer Cells. Biomolecules. 2022; 12:1360.
https://doi.org/10.3390/biom12101360
PMID:36291568

61. Hoang DH, Buettner R, Valerio M, Ghoda L, Zhang B, Kuo YH, Rosen ST, Burnett J, Marcucci G, Pullarkat V, Nguyen LX. Arsenic Trioxide and Venetoclax Synergize against AML Progenitors by ROS Induction and Inhibition of Nrf2 Activation. Int J Mol Sci. 2022; 23:6568.
https://doi.org/10.3390/ijms23126568
PMID:35743010

62. Daye M, Belviranli M, Okudan N, Mevlitoglu I, Oz M. The effect of isotretinoin therapy on oxidative damage in rats. Dermatol Ther. 2020; 33:e14111.
https://doi.org/10.1111/dth.14111
PMID:32737933

63. Bagegni NA, Park H, Kraft K, O-Toole M, Gao F, Waqar SN, Ratner L, Morgensztern D, Devarakonda S, Amin M, Baggstrom MQ, Liang C, Selvaggi G, et al. Phase 1b trial of anti-VEGF/PDGFR vorolanib combined with immune checkpoint inhibitors in patients with advanced solid tumors. Cancer Chemother Pharmacol. 2022; 89:487–97.
https://doi.org/10.1007/s00280-022-04406-6
PMID:35247086

64. Proietti I, Skroza N, Michelini S, Mambrin A, Balduzzi V, Bernardini N, Marchesiello A, Tolino E, Volpe S, Maddalena P, Di Fraia M, Mangino G, Romeo G, Potenza C. BRAF Inhibitors: Molecular Targeting and Immunomodulatory Actions. Cancers (Basel). 2020; 12:1823.
https://doi.org/10.3390/cancers12071823
PMID:32645969

65. Thomazini BF, Lamas CA, Dolder MA. Safety of isotretinoin treatment as measured by liver parameters. Histol Histopathol. 2019; 34:755–63.
https://doi.org/10.14670/HH-18-075
PMID:30556579

66. Shin HJ, Kwon HK, Lee JH, Anwar MA, Choi S. Etoposide induced cytotoxicity mediated by ROS and ERK in human kidney proximal tubule cells. Sci Rep. 2016; 6:34064.
https://doi.org/10.1038/srep34064
PMID:27666530

67. He PJ, Ge RF, Mao WJ, Chung PS, Ahn JC, Wu HT. Oxidative stress induced by carboplatin promotes apoptosis and inhibits migration of HN-3 cells. Oncol Lett. 2018; 16:7131–8.
https://doi.org/10.3892/ol.2018.9563
PMID:30546448

68. Jilani K, Lang F. Carmustine-induced phosphatidylserine translocation in the erythrocyte membrane. Toxins (Basel). 2013; 5:703–16.
https://doi.org/10.3390/toxins5040703
PMID:23604064